FUNDAMENTAL PRINCIPLES OF STRUCTURAL BEHAVIOUR UNDER THERMAL EFFECTS

A.S.Usmani and J.M. Rotter
School of Civil and Environmental Engineering, University of Edinburgh

Keywords: Composite structures, thermal expansion, thermal bowing, restraint to thermal actions, non-linear geometrical responses.

Abstract

Behaviour of composite structures in fire has long been understood to be dominated by the effects of strength loss caused by thermal degradation and that large deflections and run-away resulting from the action of imposed loading on a 'weakened' structure. Thus 'strength' and 'loads' are quite generally believed to be the key factors determining structural response (fundamentally no different from ambient behaviour). The exceptional longevity of this view derives in no small measure from observations in the standard fire tests. These observations have little relevance to realistic structural configurations present in large multi-storey composite frame structures. The investigations as part of the DETR, PIT project on composite structure behaviour in fire has clearly shown that this understanding is gravely in error. A 'new understanding' has been produced from the PIT project, sponsored by DETR (UK) and executed by a consortium led by Edinburgh University and including British Steel (now CORUS) and Imperial College. The key message from this new understanding is that, composite framed structures of the type tested at Cardington possess enormous reserves of strength through adopting large displacement configurations, and that thermally induced forces and displacements, not material degradation, govern the response in fire. Degradation (mainly steel yielding and buckling) can even be helpful in developing the large displacement load carrying modes safely. This paper attempts to lay down some of the most important and fundamental principles that govern the behaviour of composite frame structures in fire in a simple and comprehensible manner. This is based upon the analysis of the response of single structural elements under a combination of thermal actions and end restraints representing the surrounding structure.

1 Introduction

The assessment of the adequacy of composite steel frame structures in fire continues to be based upon the performance of isolated elements in standard furnace tests. This is despite the widespread acceptance amongst structural engineers that such an approach is over-conservative and even more importantly, *unscientific*. Current codes such as BS 5950 Part 8 and EC3 (draft) allow designers to take advantage of the most recent developments in the field by treating fire related loading as another limit state. The advances in understanding of structural behaviour in fire achieved in the last few years have been considerable. In theory, these advances make it possible for designers to treat the design for fire in an integrated manner with the design of a structure for all other types of loading by using the numerical modelling tools that have been instrumental in developing this understanding. However the use of such tools, which are indispensable for research, is not practical in the design office. Exploitation of the new knowledge can only become feasible if this understanding is further developed into simpler analytical expressions, enabling consulting engineers and designers to undertake performance-based design of steel frame structures without having to resort to large scale computation.

This paper builds upon earlier work presented at the INTERFLAM [1] and SiF [2] conferences. The most fundamental relationship that governs the behaviour of structures when subjected to

thermal effects is:

$$\varepsilon_{total} = \varepsilon_{thermal} + \varepsilon_{mechanical}$$

$$\text{with} \qquad \varepsilon_{mechanical} \rightarrow \sigma \qquad \text{and} \qquad \varepsilon_{total} \rightarrow \delta \tag{1}$$

The total strains govern the deformed shape of the structure δ, through kinematic or compatibility considerations. By contrast, the stress state in the structure σ (elastic or plastic) depends only on the mechanical strains.

Where the thermal strains are free to develop in an unrestricted manner and there are no external loads, axial expansion or thermal bowing results from

$$\varepsilon_{total} = \varepsilon_{thermal} \qquad \text{and} \qquad \varepsilon_{total} \rightarrow \delta \tag{2}$$

By contrast, where the thermal strains are fully restrained without external loads, thermal stresses and plastification result from

$$0 = \varepsilon_{thermal} + \varepsilon_{mechanical} \qquad \text{with} \qquad \varepsilon_{mechanical} \rightarrow \sigma \tag{3}$$

The single most important factor that determines a real structures response to heating is the manner in which it responds to the unavoidable thermal strains induced in its members through heating. These strains take the form of thermal expansion to an increased length (under an average centroidal temperature rise) and curvature (induced by a temperature gradient through the section depth). If the structure has insufficient end translational restraint to thermal expansion, the considerable strains are taken up in expansive displacements, producing a displacement-dominated response. Thermal gradients induce curvature leading to bowing of a member whose ends are free to rotate, again producing large displacements (deflections).

Members whose ends are restrained against translation produce opposing mechanical strains to thermal expansion strains and therefore large compressive stresses (see Equation 1). Curvature strains induced by the thermal gradient in members whose ends are rotationally restrained can lead to large hogging (negative) bending moments throughout the length of the member without deflection. The effect of induced curvature in members whose ends are rotationally unrestrained, but translationally restrained, is to produce tension.

Therefore for the same deflection in a structural member a large variety of stress states can exist; large compressions where restrained thermal expansion is dominant; very low stresses where the expansion and bowing effects balance each other; in cases where thermal bowing dominates, tension occurs in laterally restrained and rotationally unrestrained members, while large hogging moments occur in rotationally restrained members. This variety of responses can indeed exist in real structures if one imagines the many different types of fire a structure may be subjected to. A fast burning fire that reaches flashover and high temperatures quickly and then dies off can produce high thermal gradients (hot steel and relatively cold concrete) but lower mean temperatures. By contrast, a slow fire that reaches only modest temperatures but burns for a long time could produce considerably higher mean temperature and lower thermal gradients.

Most situations in real structures under fire have a complex mix of mechanical strains due to applied loading and mechanical strains due to restrained thermal expansion. These lead to combined mechanical strains which often far exceed the yield values, resulting in extensive plastification. The deflections of the structure, by contrast, depend only on the total strains, so these may be quite small where high restraint exists, but they are associated with extensive plastic straining. Alternatively, where less restraint exists, larger deflections may develop, but with a lesser demand for plastic straining and so less destruction of the stiffness properties of the materials. These relationships, which indicate that larger deflections may reduce material damage and correspond to

higher stiffnesses, or that restraint may lead to smaller deflections with lower stiffnesses, can produce structural situations which appear to be quite counter-intuitive if viewed from a conventional (ambient) structural engineering perspective.

The ideas presented above will be more formally explored in the following sections in the context of simple structural configurations and analytical expressions will be developed for many cases of fundamental importance.

2 Standard fire test and runaway failures

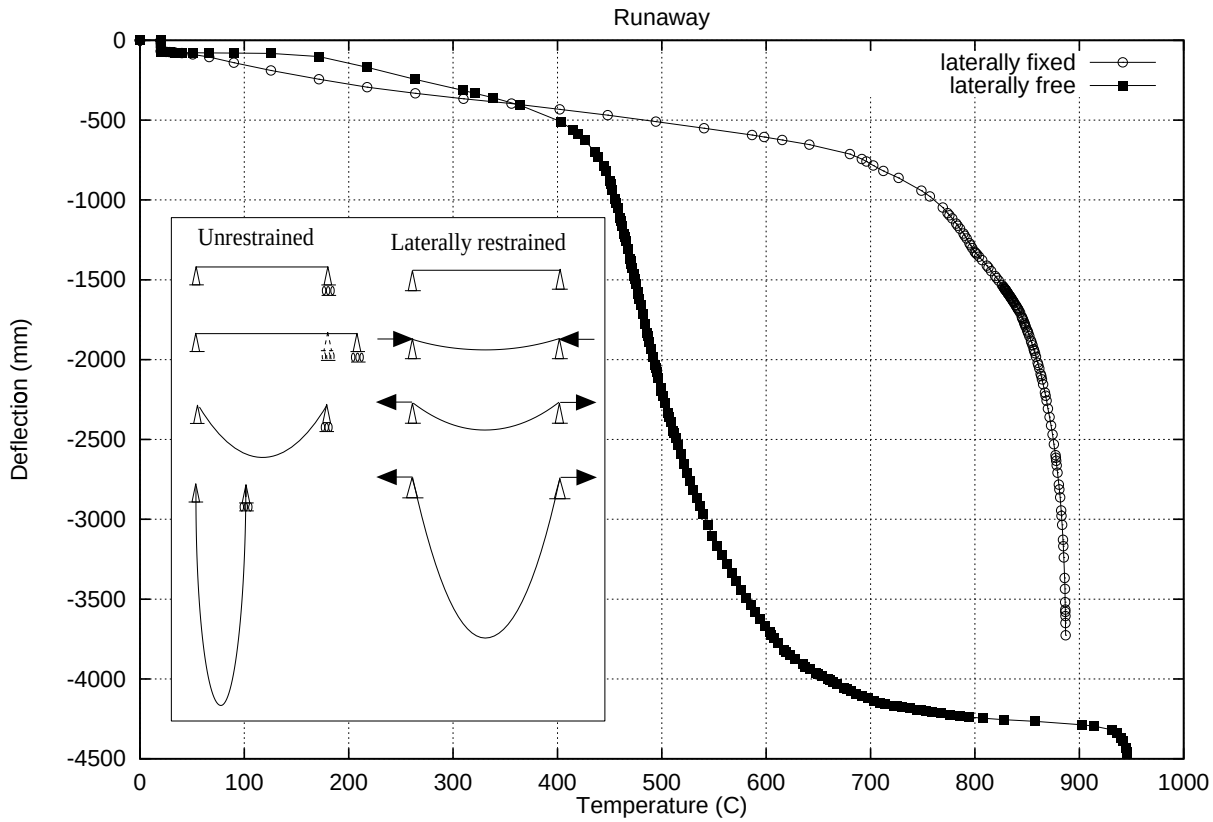

Figure 1: Runaway in unrestrained and restrained beams

Figure 1 shows a simple comparison of two geometrically non-linear analyses. The first case is heated, simply supported (laterally unrestrained) steel beam with a uniformly distributed load and the second is a laterally restrained (but rotationally unrestrained) beam with the same uniformly distributed load. Initial deflections are lower in the first beam because the supports are able to translate outwards upon expansion. However, 'runaway' occurs at around 450°C (even though considerable steel strength remains) mainly because of pulling in of the supports when the flexural stiffness of the beam reduces to a point where it cannot sustain the imposed load and there is nothing to restrain the growing deflections. In the second beam larger initial deflections occur because the beam 'buckles' due to the restraining forces very early on (70°C) and further increases in length due to thermal expansion can only be accommodated in deflection. But runaway does not occur until much later (800°C) when the steel properties are completely lost. This illustrates that the presence of restraints to end translation delays 'runaway' to much higher temperatures because of development of catenary action to replace the highly depleted flexural stiffness.

The second beam is a much more appropriate model for beams in large redundant structures. In real structures not only is this restraint available but the steel beam is in composite action with the

concrete slab which produces a much stronger and more robust structure. This strength and robustness is enhanced by the redistribution mechanisms present in redundant structures (for instance the load may be carried by the transverse slab supported in tensile membrane action which retains its strength for much longer than the steel beams). Large deflections seen in real structures are often misinterpreted as impending runaway failure. Figure 1 clearly shows that for temperatures below 300°C, the deflections for the restrained beam are much larger than that for the simply supported beam, however they have nothing to do with runaway. These deflections are caused entirely by the increased length of the beam through thermal expansion and are not a sign of loss of 'strength' or 'stiffness' in the beam until much later. In fact approximately 90% of the deflection at 500°C and 75% at 600°C is explained by thermal expansion alone. Most of the rest is explained by increased strains due to reduced modulus of elasticity. However the behaviour remains stable until about 700°C when the first signs of runaway begin to appear.

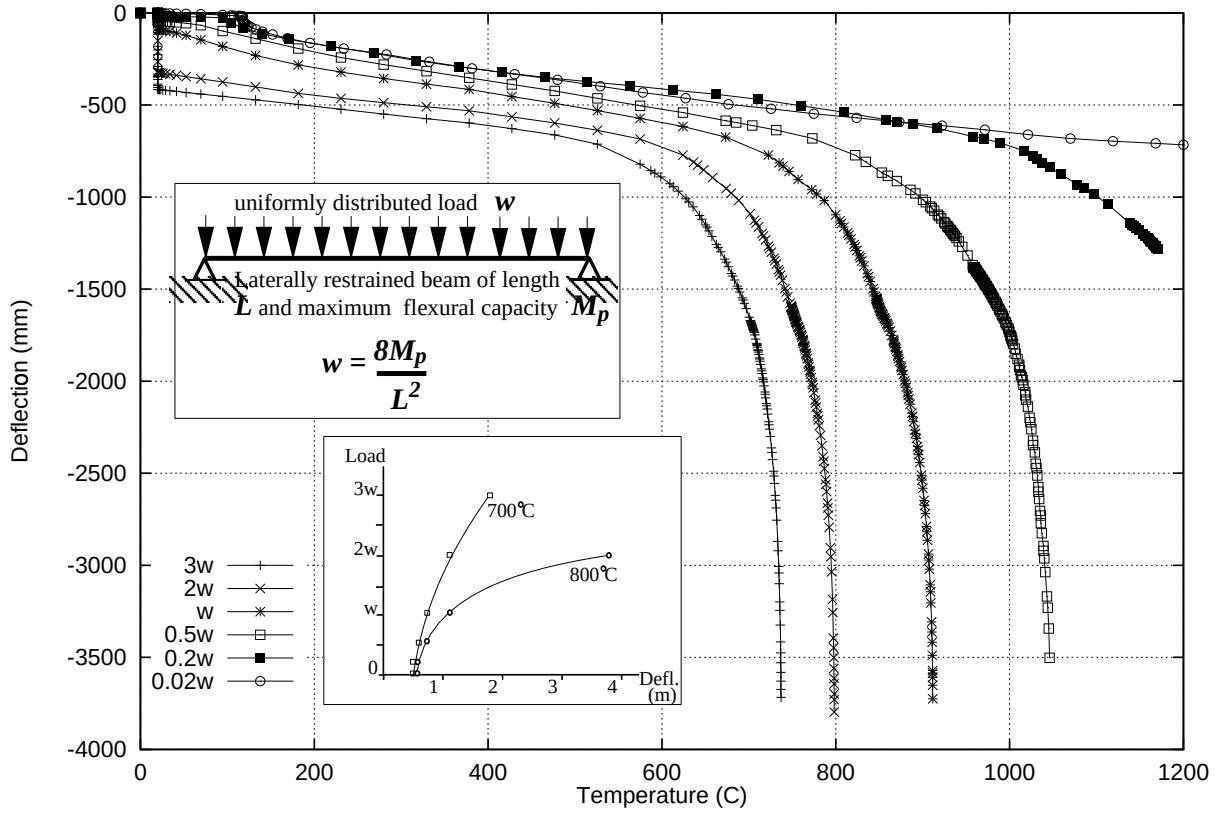

Figure 2: Effect of increasing loads on runaway in a restrained beam

Figure 2 shows another interesting analysis, where the same laterally restrained beam (as in Figure 1) has been loaded with different magnitudes of uniformly distributed load (w) in proportion to the udl that will cause a plastic hinge to occur at midspan. The Figure clearly shows that tensile membrane (or catenary) action allows loads much larger that the *ultimate* to be supported to very high temperatures. It also shows that deflections (plotted at midspan) remain insensitive to the load until just before runaway. This is true even for the case of high loads (2*w* and 3*w*) where the initial deflections before heating are already very large indicating that tensile membrane action is being exploited. The difference between the midspan deflection for the lowest load (0.02*w*) against the highest load (3*w*) stays practically constant upto approximately 600°C, indicating that upto this temperature the imposed loads have little effect on the response of the structure, which is almost completely governed by the thermal actions. Just before runaway failure, the loads begin to exert a much greater influence on the weakened structure. The temperature at which runaway eventually occurs, is sensitive to the magnitude of load. The inset graph shows the change in load against deflection for two temperatures, where reducing slope indicates runaway.

3 Thermal expansion

Heating induces thermal expansion strains (say ε_T) in most structural materials. These are given by,

$$\varepsilon_T = \alpha \Delta T \tag{4}$$

If a uniform temperature rise, ΔT, is applied to a simply supported beam without axial restraint, the result will simply be an expansion or increase in length of $l\alpha\Delta T$ as shown in Figure 3. Therefore the total strain (say ε_t) is equal to the thermal strain and there is no mechanical strain (say ε_m) which means that no stresses develop in the beam.

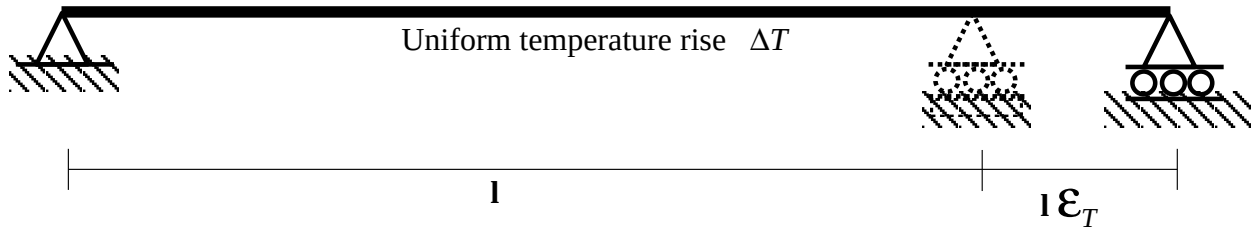

Figure 3: Uniform heating of a simply supported beam

3.1 Thermal expansion against rigid lateral restraints

Clearly beams in a real structures do not have the freedom to elongate in the manner described above. Therefore a more realistic case is to consider an axially restrained beam subjected to a uniform temperature rise, ΔT (as shown in Figure 4). It is clear to see that in this case the total strain ε_t is zero (no displacements). This is because the thermal expansion is cancelled out by equal and opposite contraction caused by the restraining force P (*i.e.* $\varepsilon_t = \varepsilon_T + \varepsilon_m = 0$ therefore $\varepsilon_T = -\varepsilon_m$). There exists now a uniform axial stress σ in the beam equal to $E\varepsilon_m$. The magnitude of the restraining force P is,

$$P = EA\varepsilon_m = -EA\varepsilon_T = -EA\alpha\Delta T$$

Figure 4: Axially restrained beam subjected to uniform heating

If the temperature is allowed to rise indefinitely, there are two basic responses, depending upon the slenderness of the beam:

1 If the beam is sufficiently stocky the axial stress will sooner or later reach the yield stress σ_y of the material and if the material has an *elastic-plastic* stress-strain relationship, the beam will continue to yield without any further increase in stress, but it will also store an increasing magnitude of *plastic strains*. The *yield temperature increment* ΔT_y is,

$$\Delta T_y = \frac{\sigma_y}{E\alpha}$$

2 If the beam is slender then it will buckle before the material reaches its yield stress. The Euler buckling load P_{cr} for a beam/column as in Figure 4 is,

$$P_{\text{cr}} = \frac{\pi^2 EI}{l^2}$$

equating this to the restraining force P, we have,

$$EA\alpha\Delta T = \frac{\pi^2 EI}{l^2}$$

which leads to a critical buckling temperature of,

$$\Delta T_{\text{cr}} = \frac{\pi^2}{\alpha}\left(\frac{r}{l}\right)^2 \tag{5}$$

or

$$\Delta T_{\text{cr}} = \frac{\pi^2}{\alpha\lambda^2} \tag{6}$$

where r is the radius of gyration and λ is the slenderness ratio ($\frac{l}{r}$). This expression is valid for other end-restraint conditions if l is interpreted as the *effective length*.

In this case, if the temperature is allowed to rise further, the total restraining force will stay constant (assuming elastic material and no thermal degradation of properties) and the thermal expansion strains will continue to be accommodated by the outward deflection of the beam δ as shown in Figure 5.

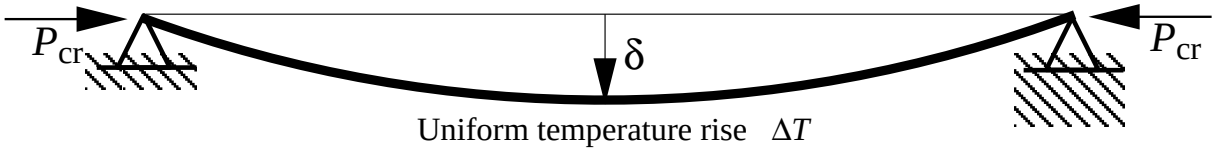

Figure 5: Buckling of an axially restrained beam subjected to uniform heating

The above cases represent the two fundamental responses in beams subjected to restrained thermal expansion. Either of the two (yielding or buckling) may occur on its own (based upon the slenderness of the beam) or a more complex response consisting of a combination of yielding and buckling may occur.

The pattern of development of deflections, axial compression forces and moments with increase in temperature in slender restrained elastic beams is as shown in Figures 6and 7. The deflection and axial force figures clearly show a pre-buckling and post-buckling type response. The sharp bifurcation pattern is absent as a uniformly distributed load is imposed on the beam, imparting an initial displacement to it. The midspan moment continues to rise even after buckling as it consists mainly of the $P - \delta$ moment generated by the axial restraint force times the midspan deflection (which continues to rise beyond buckling).

Ideal elastic properties were assumed when discussing the case of buckling above. If the properties are ideal elasto-plastic the deflections and axial compression variations will have a pattern as shown in Figure 8. If the properties remain elastic albeit with a uniform degradation with temperature, the pattern of deflection and axial compression in the beam changes to the one shown in Figure 9. Clearly the response of real composite beams subject to restrained thermal expansion will consist of a combination of the responses shown here. That this is indeed the case, can be seen in report AM1, where the results of modelling the British Steel *restrained beam* Test are shown (which comes closest to the ideal case of rigid lateral restraint). There are other factors in that Test that govern the response of the heated composite beam, particularly the effect of deflection compatibility in the two directions, however the similarity of the development of axial forces in the steel joist and the composite beam to the patterns shown here is clear to see.

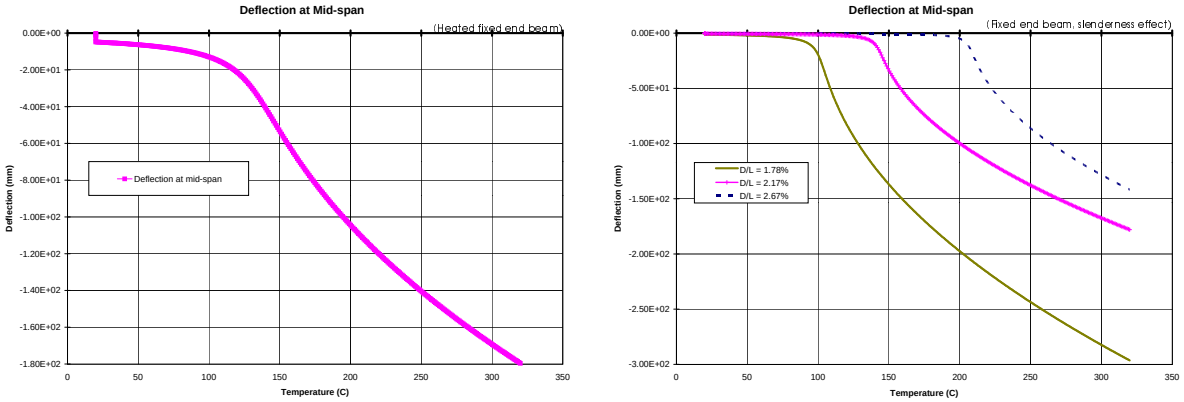

(a) **(b)**

Figure 6: Deflection of axially restrained elastic beams subjected to heating: (a) Single beam, (b) Three beams of varying slenderness

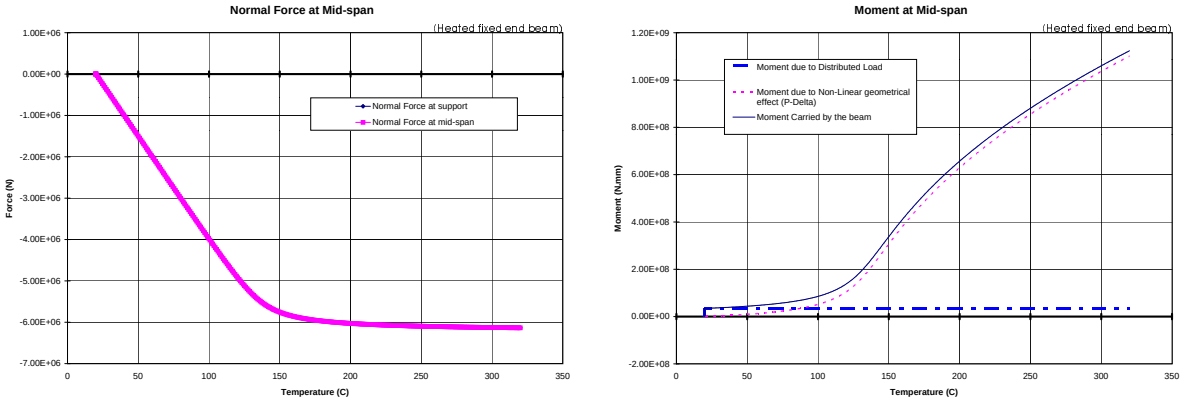

(a) **(b)**

Figure 7: Forces in an axially restrained elastic beam subjected to heating: (a) Axial Forces, (b) Moments

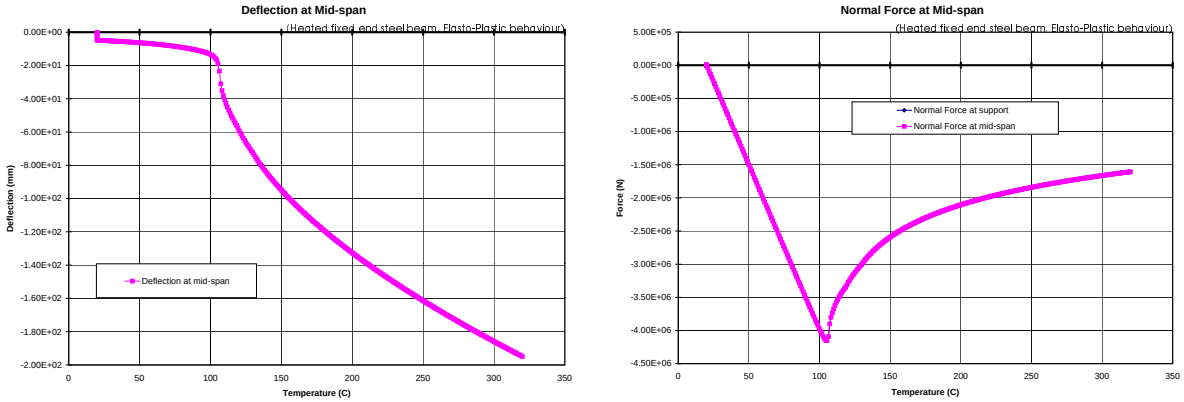

(a) **(b)**

Figure 8: Deflections (a), & Axial forces (b), in an axially restrained elastic-plastic beam

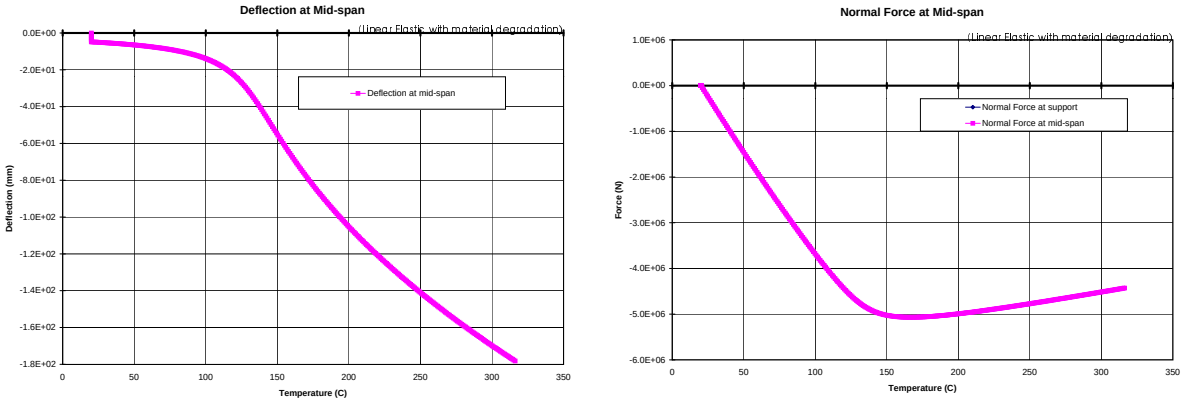

(a) **(b)**

Figure 9: Deflections (a), & Axial forces (b), in a restrained beam with reducing elastic stiffness

3.2 Thermal expansion against finite lateral restraints

In the previous discussion we have assumed the axial restraints to be perfectly rigid. This is an upper limit and practically impossible to achieve in real structures which offer only finite restraints. Figure 10 shows such a beam restrained axially by a translational spring of stiffness k_t. The compressive axial stress developed by thermal expansion is,

$$\sigma = \frac{E\alpha\Delta T}{\left(1+\frac{EA}{k_t L}\right)} \tag{7}$$

and critical buckling temperature is now given by,

$$\Delta T_{\text{cr}} = \frac{\pi^2}{\alpha\lambda^2}\left(1+\frac{EA}{k_t L}\right) \tag{8}$$

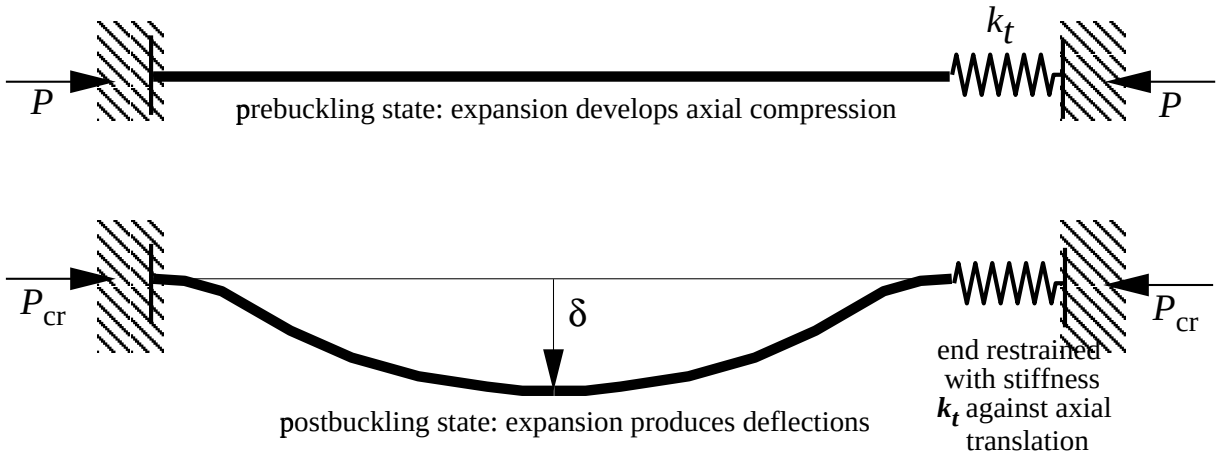

Figure 10: Heating of beam with finite axial restraint

From Equation 8 it can be seen that buckling and post-buckling phenomena should be observable at moderate fire temperatures in structures with translational restraint stiffnesses (k_t) which are quite comparable with the axial stiffness of the member ($\frac{EA}{L}$). Figure 11 shows a plot derived from Equation 8, where critical buckling temperatures are plotted against slenderness ratio for different restraint stiffnesses. The results clearly show that the amount of restraint required is not large for slender sections to reach buckling temperature. Bearing in mind that the axial stiffness

of the member ($\frac{EA}{L}$) itself is reduced by heating through the reduction in E, so these post-buckling phenomena are **very likely** to be observed in beams in typical fires.

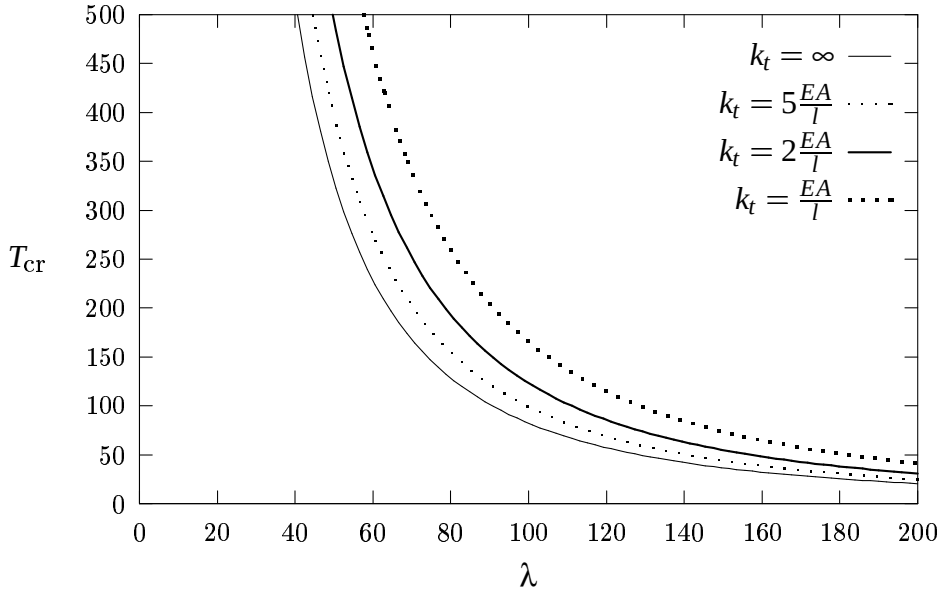

Figure 11: Buckling temperatures for thermal expansion against finite lateral restraint

4 Thermal bowing

In the previous section we discussed the effects of uniform temperature rise on axially restrained beams. In real fires the temperature distributions are anything but uniform. In a small to moderate size compartment of a regular shape one may assume that the compartment temperature will be roughly uniform at a given time. The temperature of the structural members in the compartment depends upon the material they are made of and other details of geometry, construction and design (such as insulation). Concrete beams and slabs on the ceiling of the compartment can be subjected to very high temperature gradients due to the very slow rates of heat transfer to concrete. Therefore the surfaces exposed to fire will be at a much higher temperature than the surfaces on the outside of the compartment. This causes the inner surfaces to expand much more than the outer surfaces inducing bending in the member. This effect is called *thermal bowing* and is one of the main reasons of the deformations of concrete slabs and masonry walls in fires. Another very important source of thermal bowing in composite beams/slabs is the large difference between the temperatures of the steel joist and the slab. This effect is much more important in the early stages of the fire when steel retains most of its strength.

Relationships can be derived for thermal bowing analogous to the one derived earlier for thermal expansion. Figure 12 shows a beam subjected to a uniform temperature gradient through its depth (d) along its whole length (l). Assuming the beam is simply supported (as shown in Figure 12) we can derive the following relationships:

1 The thermal gradient (T_y) over the depth is,

$$T_y = \frac{T_2 - T_1 1}{d}$$

2 A uniform curvature (ϕ) is induced along the length as a result of the thermal gradient,

$$\phi = \alpha T_y$$

3 Due to the curvature of the beam the horizontal distance between the ends of the beam will reduce. If this reduction is interpreted as a contraction strain (not literally) ε_ϕ (analogous to the thermal expansion strain ε_T earlier), the value of this strain can be calculated from analysing Figure 12 as:

$$\varepsilon_\phi = 1 - \frac{\sin\frac{l\phi}{2}}{\frac{l\phi}{2}} \tag{9}$$

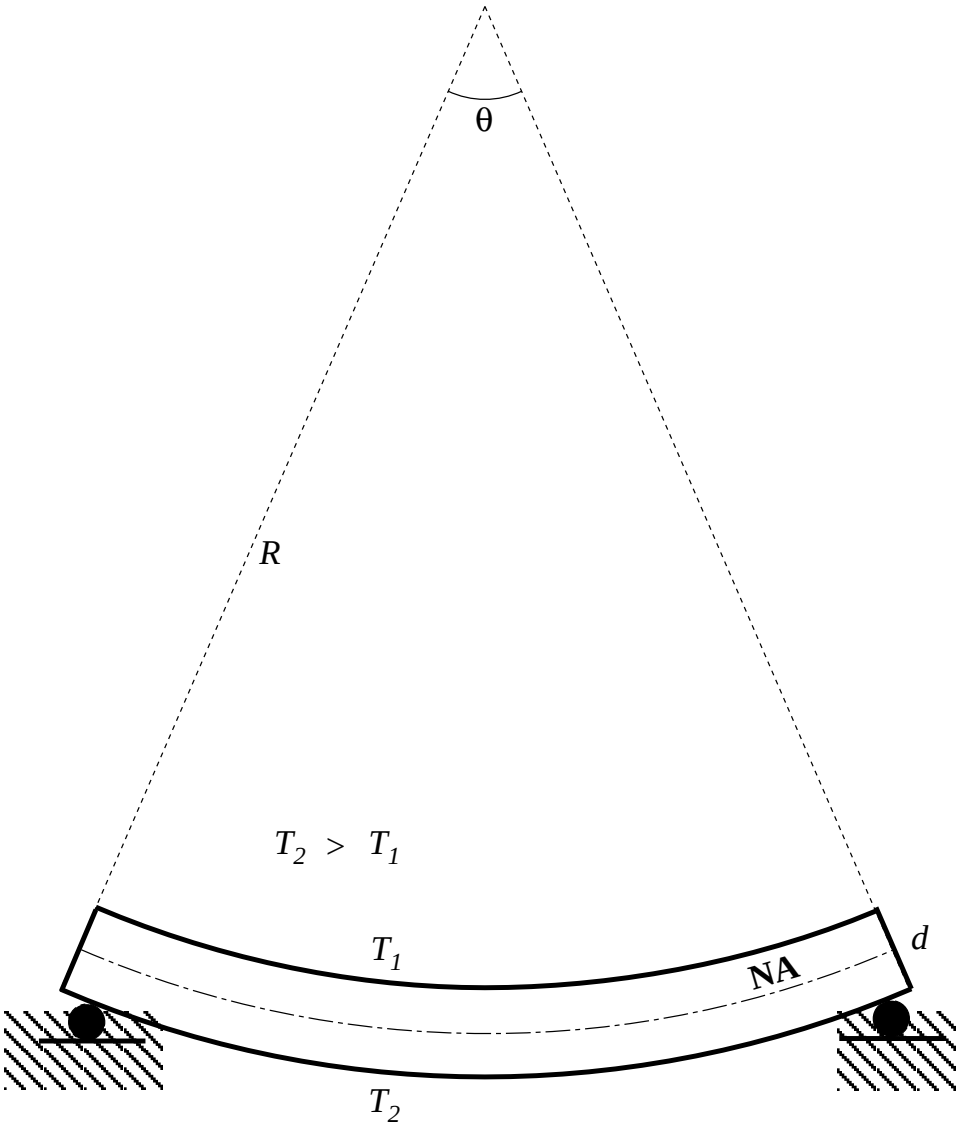

Figure 12: Simply supported beam subjected to a uniform thermal gradient

Now consider the laterally restrained beam of Figure 5. If a uniform thermal gradient T_y is applied to this beam (as shown in Figure 13), the result (in the absence of any average rise in temperature, *i.e.* mean temperature remaining constant) is a thermally induced tension in the beam and corresponding reactions at the support (opposite the the pure thermal expansion case discussed earlier). This is clearly caused by the restraint to end translation against the contraction strain (ε_ϕ) induced by the thermal gradient.

Figure 14 shows a fixed ended beam (by adding end rotational restraints to the Beam of Figure 13) subjected to a uniform temperature gradient through its depth. Recalling that a uniform curvature $\phi = \alpha T_y$ exists in a simply supported beam subjected to gradient T_y. If that beam is rotationally restrained by support moments M (uniform along length) an equal and opposite curvature induced

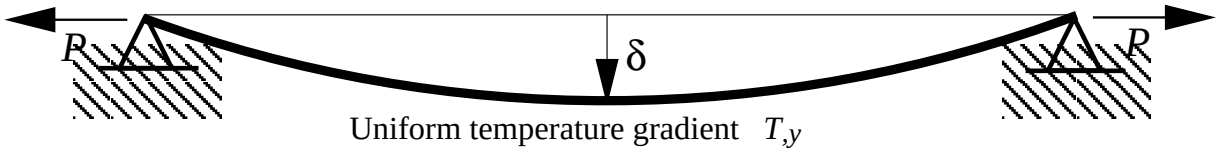

Figure 13: Laterally restrained beam subjected to a uniform thermal gradient

by the support moments cancels out the thermal curvature and therefore the fixed ended beam remains 'straight' with a constant moment $M = EI\phi$ along its length.

Figure 14: Fixed end beam subjected to a uniform thermal gradient

From the above discussion it is clear that the effect of boundary restraints is crucial in determining the response of structural members to thermal actions. The key conclusion to be drawn from the discussion so far is that, *thermal strains will be manifested as displacements if they are unrestrained or as stresses if they are restrained through counteracting mechanical strains generated by restraining forces*.

As discussed earlier for lateral restraint, perfect rotational restraint is also not very easily achieved in real structures (other than for symmetric loading on members over continuous supports, without any *hinges* from strength degradation). Figure 15 shows a beam restrained rotationally at the ends by rotational springs of stiffness k_r. In this case the restraining moment in the springs as a result of a uniform thermal gradient $T_{,y}$ can be found to be,

$$M_k = \frac{EI\alpha T_{,y}}{\left(1 + \frac{2EI}{k_r l}\right)} \tag{10}$$

This equation implies that if the rotational restraint stiffness is equal to the rotational stiffness of the beam itself ($\frac{EI}{l}$) then the moment it will attract will be about a third of a fixed support moment.

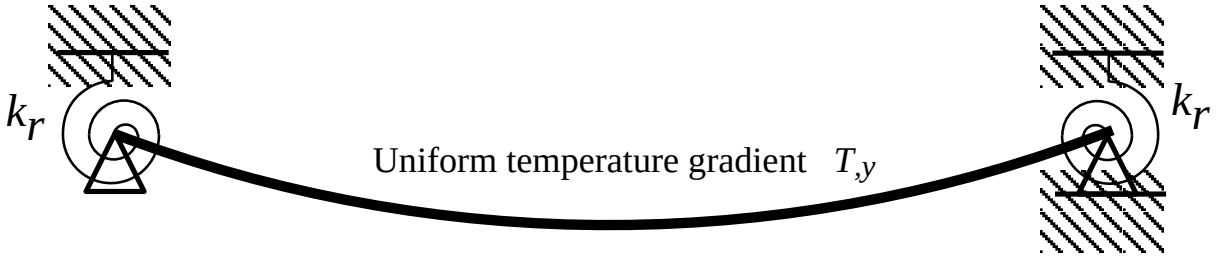

Figure 15: Beam with finite rotational restraint with a uniform thermal gradient

5 Deflections

In the previous sections we have looked at the overall behaviour of beams subjected to expansion and bowing for various restraint conditions. One interesting aspect of structural response to fire is the large deflections that are found in structural members such as beams and slabs. Large deflections are normally associated with loss of strength in structures under ambient conditions. In

case of fire such a simple interpretation can be highly misleading. Both the thermal mechanisms discussed earlier (thermal expansion and thermal bowing) result in large deflections, however the state of stress associated with a member subjected to varying degrees of these two mechanisms is not unique for a given deflection and a large range of stress states exist (large compression or tension or very low stresses) depending upon the temperature distribution in the member and its material properties and restraint conditions.

The chief reason for large deflections is that the structural member tries to accommodate the *additional length* generated by thermal expansion, given that it is not possible for it to expand longitudinally due to end restraints. Consider a slender beam (very low buckling temperature) subjected to uniform heating against rigid lateral restraints (as in Figure 5). Buckling will occur very early on (at very low elastic strains) after which any further expansion will make the beam deflect outwards. The resulting midspan deflection δ can be approximated quite accurately by,

$$\delta = \frac{2l}{\pi}\sqrt{\varepsilon_T + \frac{\varepsilon_T^2}{2}} \tag{11}$$

which is an approximation of the deflection of a sin curve of length $l(1+\varepsilon_T)$, where ε_T is the thermal expansion strain ($\alpha\Delta T$).

If the same beam is subjected to a uniform thermal gradient producing no net expansion, only bowing as in Figure 13, the response is then determined by the flexure-tension interaction. The tensile $P-\delta$ moments restrain the curvature imposed by the thermal gradients and limit deflections. The deflections result from the tensile strains produced in the beam, *i.e.*

$$\varepsilon_t = \frac{P}{EA} \tag{12}$$

and the deflections can then be determined by

$$\delta = \frac{2l}{\pi}\sqrt{\varepsilon_t + \frac{\varepsilon_t^2}{2}} \tag{13}$$

The tensile force P_t can be determined from substituting Equation 12 in Equation 13 and solving a quadratic equation for P_t,

$$P_t = \left(\sqrt{\frac{1}{2}\left(\frac{\pi\delta}{l}\right)^2 + 1} - 1\right) EA \tag{14}$$

To determine the deflection $y(x)$ in the beam of Figure 13 for a given curvature ϕ (arising from a thermal gradient), a differential equation solution can be written as follows:

For a simply supported beam subjected to a uniform curvature ϕ one can write,

$$\frac{d^2y}{dx^2} = \phi$$

If the beam is laterally restrained as in Figure 13, a tensile force P will be generated causing a moment Py over the length of the beam, therefore,

$$\frac{d^2y}{dx^2} = \phi + \frac{Py}{EI} \tag{15}$$

or

$$\frac{d^2y}{dx^2} - k^2y = \phi$$

where,

$$k = \sqrt{\frac{P}{EI}}$$

The solution of this equation is,

$$y(x) = -\frac{\phi}{k^2}\left(\frac{\cosh kl - 1}{\sinh kl}\sinh kx - \cosh kx + 1\right) \tag{16}$$

It may be seen that Equations 14 and 16 form a set of nonlinear equations. These equations can be solved using an appropriate iterative technique (bisection, Newton-Raphson) to obtain the tensile forces and deflections for thermal gradient dominated problems.

6 Combinations of thermal expansion and thermal bowing

In the previous sections the response of beams to either thermal expansion or thermal bowing have been considered in isolation. To study the combined response let us first consider the case of a fixed ended beam as shown in Figure 16 which is both rotationally and translationally restrained at both ends. If this beam is subjected to a mean temperature rise and a through depth thermal gradient, it will experience a uniform compressive stress because of restrained expansion and a uniform moment because of the thermal gradient. The stresses on any typical cross-section because of the combined effect of the two thermal actions are also shown in Figure 16. It is clear that the bottom of

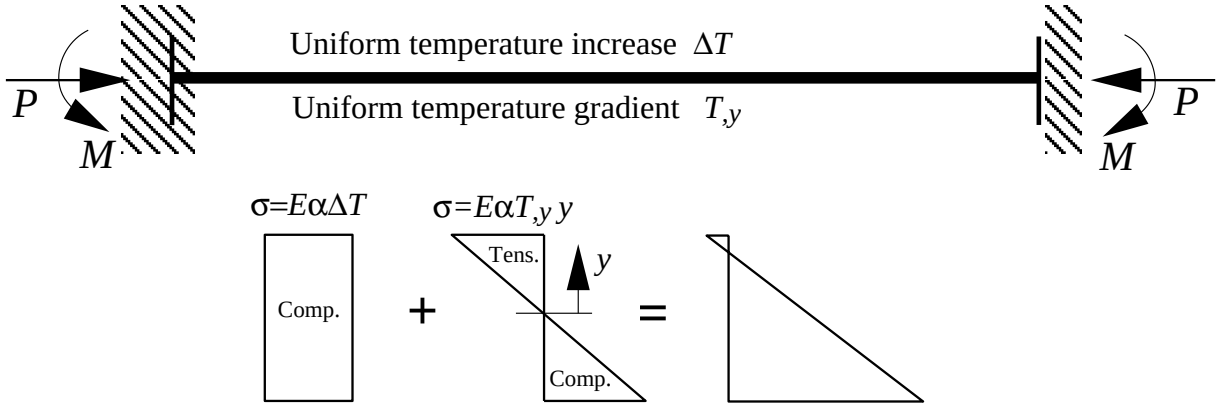

Figure 16: Combined thermal expansion and bowing in a fixed ended beam

the beam will experience very high compressive stresses, while the top may be anywhere between significant compression to significant tension.

The above scenario is a common one in composite frame structures such as Cardington. The composite action of a steel joist, framing into an interior column, with a continuous slab over it, produces conditions very close to a fully fixed support (as in Figure 16). The high compressions resulting from the combined effect of thermal actions as described above almost invariably produce local buckling in the lower flange of the steel joist very early on in a fire. This why local buckling of the lower flanges is such a common occurrence in fires (seen in all Cardington tests and other fires).

Once local buckling has occurred the pattern of stresses at the ends of the composite beam changes. The hogging moment is relieved by the *hinge* produced by local buckling and the end restraint conditions change to the one shown in Figure 13. As this happens quite early in real fires, the end conditions described by Figure 13 are the ones that govern the behaviour of a composite beam for most of the duration of the fire.

6.1 Combined thermal expansion and bowing in laterally restrained beam

The fundamental pattern of behaviour of a beam whose ends are laterally restrained (but rotationally unrestrained, see Figure 13) subjected to thermal expansion and thermal bowing separately was established in previous sections. Restrained expansion resulted in compression and bowing resulted in tension. This helped to illustrate that two opposite stress regimes can occur depending upon the thermal regime applied, however the apparent response of the beam is the same (*i.e.* downward deflection).

To study the effects of the applying combinations of thermal expansion and thermal bowing we define and effective strain as follows,

$$\varepsilon_{\text{eff}} = \varepsilon_T - \varepsilon_\phi \tag{17}$$

The variation of ε_{eff} (for various thermal regimes) can produce a large variety of responses. Positive values of ε_{eff} imply compression (or the effect of mean temperature rise is dominant) and negative values imply tension (or the effect of thermal gradients is dominant). Figure 17 shows the variation of ε_{eff} for different values of thermal gradient when the temperature is increased from 0 to 400°C (ε_{eff} is plotted for a linear increase in gradient against temperature).

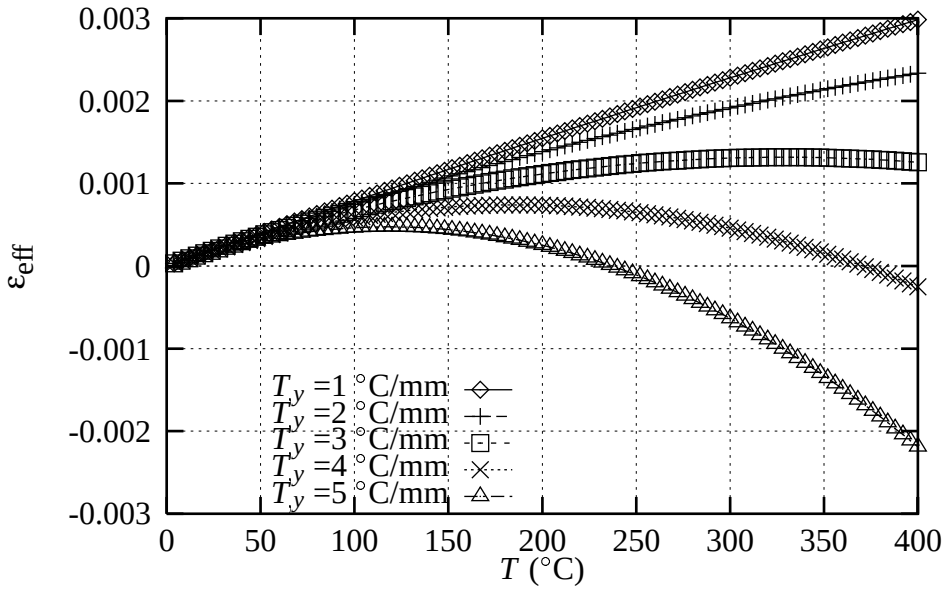

Figure 17: Effective expansion strains

Case 1: Zero stress in the beam ($\varepsilon_{\text{eff}} = 0$)

Figure 18 shows an interesting theoretical case. If the implied combination of ε_ϕ and ε_T are applied:

- There are no stresses in the beam. All thermal strains are converted into displacement as seen in the figure.
- The deflection of the beam is **entirely** due to *thermal bowing* to accommodate the *excess length* generated by expansion.
- the deflection response of this beam can be analytically expressed as the increase in length of the elastic curve of the beam versus its deflection. Figure 19 shows a number of length increase vs midspan deflection plots based on assumed curve shapes. The figure shows that the shape of the curve chosen does not matter much, therefore the formula given earlier based

Step 1 : Impose a temperature rise ΔT

Step 2 : Impose a curvature $\alpha T,_y$ to return support to the original position

Figure 18: Case 1: Zero Stress

upon the sin curve (Equation 11) can be used to get a good approximation of the midspan deflection y_m, *i.e.*

$$y_m = \frac{2l}{\pi}\sqrt{\varepsilon_T + \frac{\varepsilon_T^2}{2}}$$

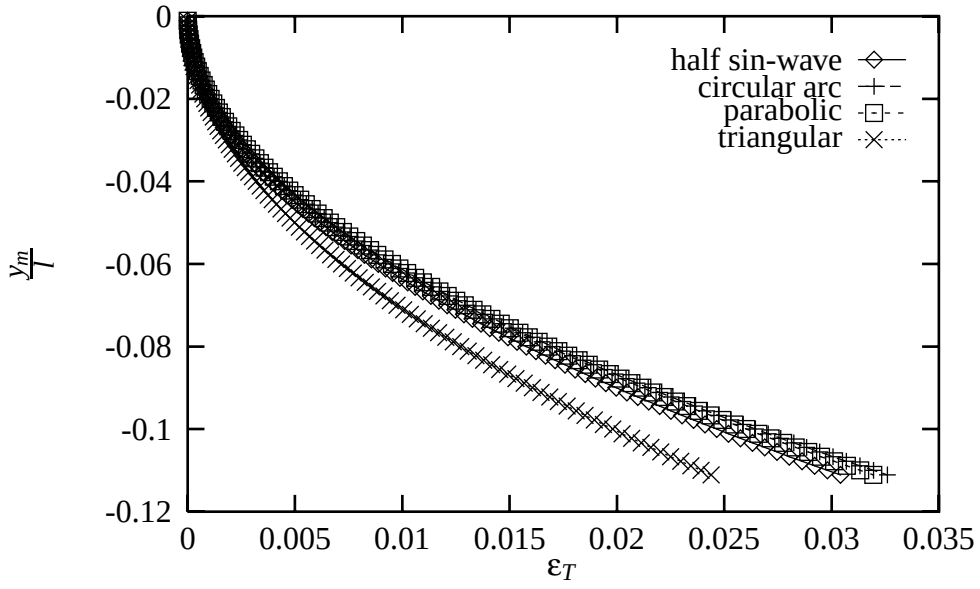

Figure 19: Strain v non-dimensional midspan deflection (per unit length)

Case 2: Thermal expansion dominant ($\varepsilon_{\text{eff}} > 0$)

If $\varepsilon_T >> \varepsilon_\phi$, thermal expansion dominates and a two stage response is produced consisting of *Pre-buckling* and *Post-buckling* phases. The thermal expansion produced is partly used up in generating mechanical strains and partly in generating deflections. This is governed by the magnitude of ε_{eff} which is the component that generates stresses to progress the beam towards buckling. The ε_ϕ component annihilates part of the expansion and produces deflections by imposing curvature with the available excess length. The pre-buckling deflections (y_m^-) will for a small part result from the elastic bending of the beam and a larger part will generally come from the deflection resulting from

the imposed curvature ($y_m(\phi)$).

$$y_m^- = \frac{y_0}{1 - \frac{\Delta T}{\Delta T_{cr}}} + y_m(\phi) \tag{18}$$

Here y_0 can be interpreted as the initial elastic deflection before the fire because of the imposed loads on the beam and $y_m(\phi)$ is the extra deflection due to thermal bowing given by,

$$y_m(\phi) = \frac{2l}{\pi}\sqrt{\varepsilon_\phi + \frac{\varepsilon_\phi^2}{2}} \tag{19}$$

The presence of the gradient clearly delays the buckling event and the critical buckling temperature (ΔT_{cr}) is increased to,

$$\Delta T_{cr} = \frac{1}{\alpha}\left(\frac{\pi^2}{\lambda^2} + \varepsilon_\phi\right) \tag{20}$$

Figure 20 shows the typical variation in buckling temperature with the change in gradient (for a beam of slenderness ratio $\frac{l}{r}$ equal to 70).

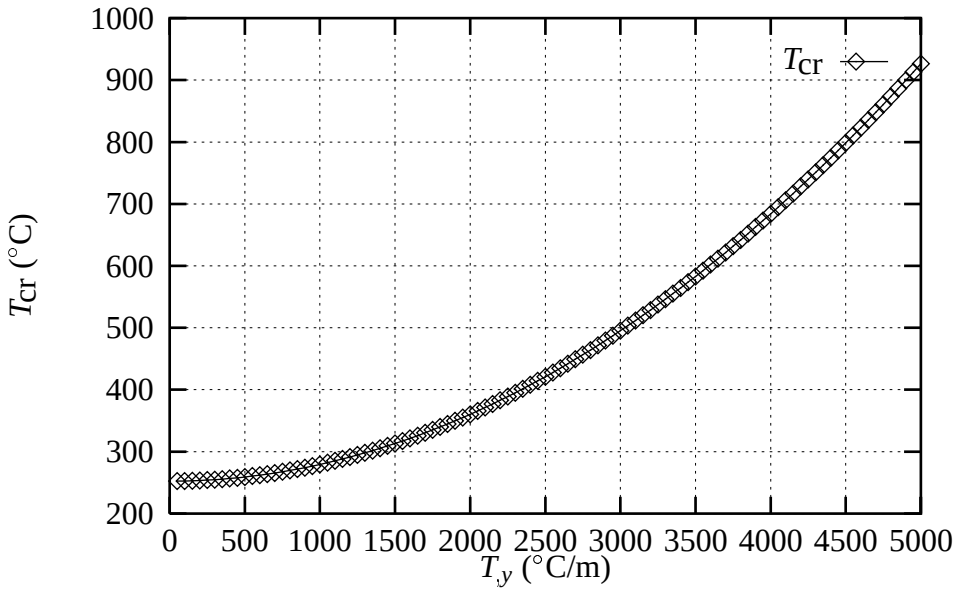

Figure 20: Critical Buckling temperatures vs Thermal gradient

The *postbuckling* deflections will carry on increasing because of all further expansion strains ε_T^+ as in Equation 11, *i.e.*

$$y_m^+ = \frac{2l}{\pi}\sqrt{\varepsilon_T^+ + \frac{\varepsilon_T^{+2}}{2}}$$

The thermal bowing deflection added to the elastic deflections (due to $P-\delta$ moments and loading) will again act as 'imperfections' to 'straightness' of the beam and produce a smooth variation of beam midspan deflection with temperature until the large displacement post-buckling mode begins (identified by the change of curvature of the temperature deflection curve). This also has the effect of reducing the development of compression forces in the beam (as the beam displaces more for lower compressions because of the additional bowing displacements increasing the $P-\delta$ moments).

Case 3: Thermal bowing dominant ($\varepsilon_{\text{eff}} < 0$)

When $\varepsilon_\phi >> \varepsilon_T$, the deflection response will be the sum of two components,

1 Deflection caused by bowing of the excess length generated through expansion, as before *i.e.*

$$(y_m)_1 = \frac{2l}{\pi}\sqrt{\varepsilon_T + \frac{\varepsilon_T^2}{2}}$$

2 The tensile strain ε_t produced by the tension (P_{eff}) caused by the excess contraction strain (ε_{eff}) as in the case of pure thermal gradients.

$$\varepsilon_t = \frac{P_{\text{eff}}}{EA}$$

which will produce further deflections as,

$$(y_m)_2 = \frac{2l}{\pi}\sqrt{\varepsilon_t + \frac{\varepsilon_t^2}{2}}$$

The tension P_{eff} and the deflections can then be determined according to the iterative procedure suggested in the previous section on deflections.

Finally Figure 21 shows the main types of deflection responses that may be observed if a laterally restrained beam is exposed to combinations of thermal actions discussed above.

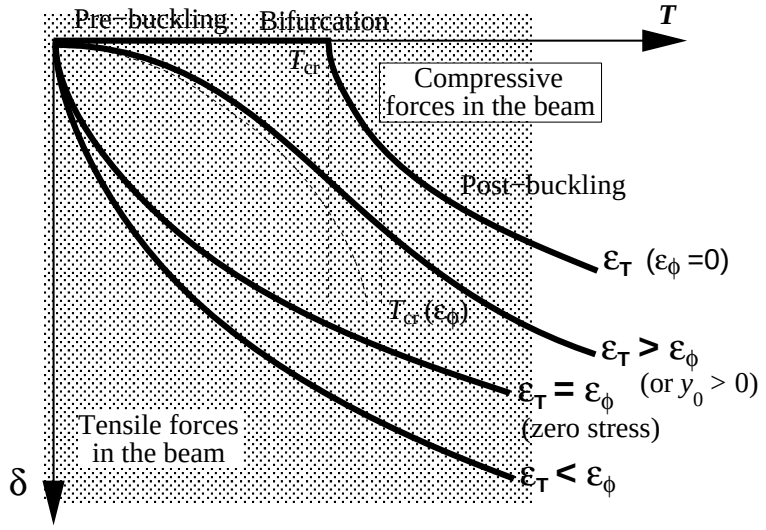

Figure 21: Temperature deflection responses for combinations of ε_T and ε_ϕ

7 Criterion for the various types of responses

From the discussion above a simple criterion for all the various types of responses observed can be developed. If ε_{eff} is close to $\frac{\pi^2}{\lambda^2}$ then there will be no buckling as not enough compression is generated. A dimensionless number ζ may be defined as follows to categorise the various responses:

$$\zeta = \frac{\varepsilon_T - \varepsilon_\phi}{\frac{\pi^2}{\lambda^2}} \tag{21}$$

To summarise,

1 $\zeta >> 1$
typically generates pre and postbuckling type deflection responses with thermal expansion and compression dominant. The compression force patterns are as discussed earlier in the restrained thermal expansion section.

2 $\zeta \simeq 1$
generates responses where most of the thermal expansion is converted into deflection but there are negligible stresses in the beam (close to the *zero stress* case discussed earlier).

3 $\zeta << 1$
generates thermal bowing dominated response with deflection patterns similar to the *zero stress* case and with considerable tensile forces in the beam which grow with the increase in the gradient.

8 Numerical analysis of the simple beam model

The analytical approach developed above to fully understand the structural response to the heating regime has been checked numerically by modelling the same simple beam examples in ABAQUS. The data for beam analysed was as follows:

- length (l)=9000 mm
- Modulus of Elasticity (E)=210000 N/mm^2
- Coefficient of thermal expansion (α)=8×10^{-6}
- Area A=5160 mm^2
- Second moment of area I =8.55×10^7 mm^2

Therefore the slenderness ratio $\frac{l}{r}$ of the beam is approximately equal to 70. This calculation is limited to investigated the simple beam model restrained laterally but free to rotate at its ends as in Figure 13. The results confirm the theoretical solutions derived for the response of the beam to thermal bowing and thermal expansion. Figure 22 shows the results of the numerical analysis in terms of the deflections and axial forces produced when the beam is subjected to a mean temperature rise (uniform over the length) of $400°C$ and an effective thermal gradient through the depth of the beam. The temperature increase, ΔT and thermal gradient, T,y were applied to the simple numerical beam model at a constant rate from zero to their maximum values. The deflection as a result of pure restrained thermal expansion shows the double curvature shape of the pre-buckling/post-buckling response (see Figure 22). When a gradient is also applied to the model and the response of the beam is governed by the interaction between thermal bowing and restrained thermal expansion the deflected shape becomes smoother, indeed for a specific combination of mean temperature rise and temperature gradient the response will be very close to linear. At large gradients ($T,y = 10°$C/mm) when the response is dominated by thermal bowing the deflected shape is very non-linear.

The corresponding axial forces are also plotted in Figure 22. When a mean temperature rise of $400°C$ alone is applied to the model and the response of the beam is governed purely by restrained thermal expansion and the axial force is in high compression. When the model is subjected to a combination of mean temperature rise and temperature gradient the axial force becomes smaller in compression and at high gradients moves into tension. The axial force at the beginning of the analysis is always in compression because the mean temperature and the gradient are applied to

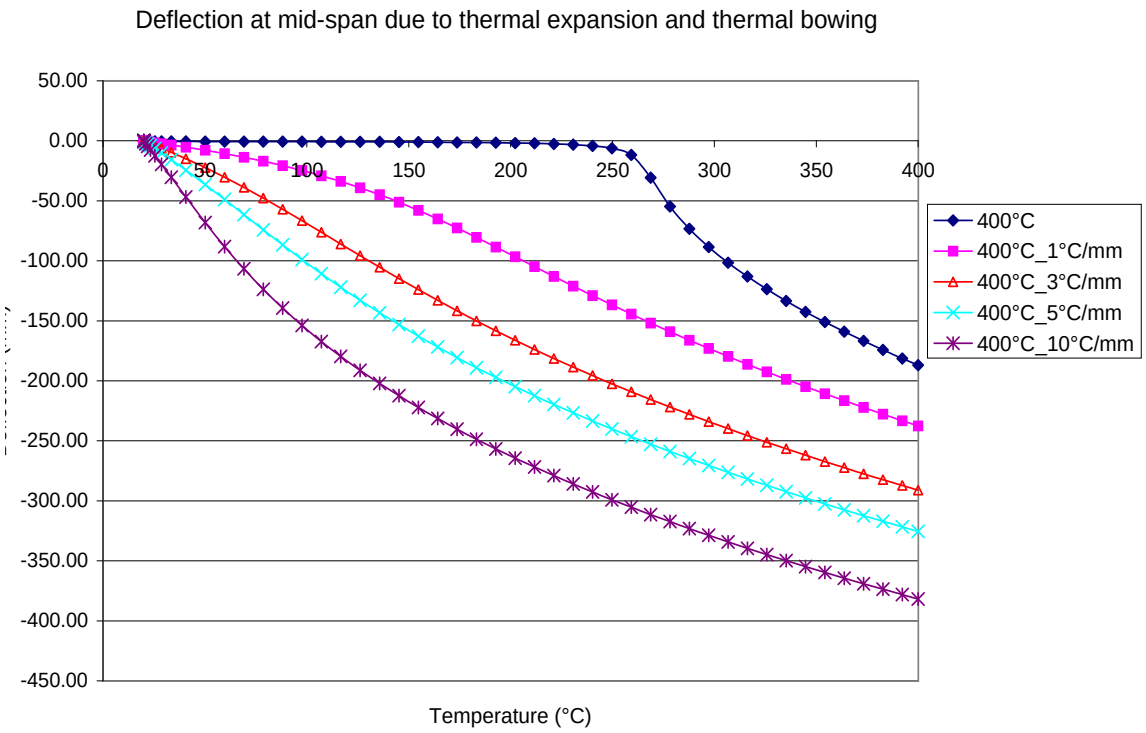

(a)

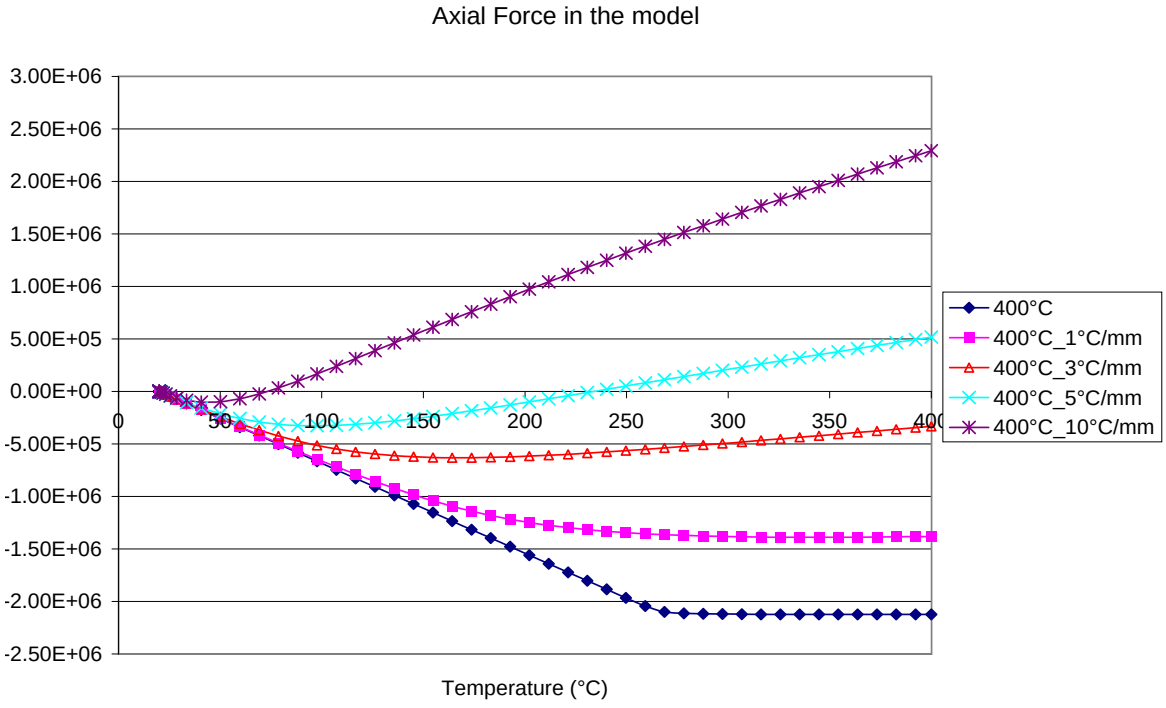

(b)

Figure 22: Numerical model results for combined thermal expansion and thermal bowing: (a) Deflections (b) Axial forces

the model linearly from zero to their maximum values and are governed by the development of the effective strains, ε_{eff}, as shown in Figure 17.

The actual values of deflections and forces in the numerical exercise above can be estimated using the formulas given here. For instance for the case of a temperature rise of $400°C$ the compression force is simply the Euler buckling load ($\frac{\pi^2 EA}{\lambda^2}$) equal to 2170 kN (approx.). The deflection for this case can be obtained from subtracting the elastic compression strain ($\frac{\pi^2}{\lambda^2}$) from the thermal strain (ε_T) to obtain the strain that produces the deflections, therefore,

$$y_m \simeq \frac{2l}{\pi}\sqrt{\varepsilon_T - \frac{\pi^2}{\lambda^2}}$$

which produces a value of approximately 200mm (within 10%) of the numerical calculation above. The difference is because the numerical calculation is fully geometrically non-linear while the above formulas are based on 1st order definitions of strain.

If all the thermal strains were to produce deflection (by appropriate combination of ε_T and ε_ϕ) then the internal forces would be very low and the deflection would be approximately 324 mm (from Equation 11) which lies between the cases of $T,y = 3°$C/mm to $T,y = 5°$C/mm. It may be noted from Figure 22 that the axial force in the beam moves from compression to tension between these values (suggesting that for the deflections in the region of 324 mm) the forces in the beam will be insignificant.

The tensile forces and deflections for large gradients can be calculated from iteratively solving the set of nonlinear Equations 14 and 16.

The above analysis clearly highlights the large range of deflected shapes and axial forces possible as a result of the interaction between thermal expansion and thermal bowing.

9 Other important factors

The discussion above has focussed upon the effects of thermal expansion and thermal bowing and illustrated the large variety of responses possible in real composite frame structures. Analytical expressions have been presented which allow a good quantitative estimate of forces and deflections to be made for simple structures.

Effects of thermal degradation and imposed loading were found to be relatively less important in the modelling of Cardington Tests (see reports SM1-2). The effect of strength degradation was shown to change the development of compressive forces in a restrained beam in Figures 8 and 9. The loading on a beam in a large displacement configuration (through thermal effects) will be carried very effectively in a *catenary* (or tensile membrane) behaviour. It is clear from the above discussion that for the most likely combinations of thermal actions (ε_T and ε_ϕ) the mechanical strains in a member are likely to be very low (compression or tension). If this is true and that thermal degradation has been contained in the surface layers, then the tensile strains induced by membrane mechanisms should be carried quite reliably. This is however an area which needs further extensive investigation using all standard research techniques, experimental, computational and theoretical.

Restraint conditions can certainly have a major effect on the distribution of the internal forces and the displacements that occur as has been illustrated by the simple theoretical and computational analyses in this paper. The degree of restraint available also changes during a fire , for instance the rotational restraint available to the composite beam at the beginning is lost quite early on (around 200 C) [3] due to the local buckling of the steel joist and tensile capacity of the slab

being reached. Rotational restraints result in increasing hogging moments until a 'plastic hinge' is achieved. Lateral translation restraints produce compression forces if thermal expansion was dominant and tension forces if thermal bowing is dominant. The amount of restraint required is not large to produce buckling as floor structures usually very slender. The source of this restraint is obvious for interior compartments - the colder and stiffer surrounding structure. For exterior compartments it is not so clear if sufficient restraints are still available. It is likely that sufficient restraint to lateral expansion is available at exterior boundaries through the actions of tension rings [1]. At large deflections lateral restraints provide an anchor to the tensile membrane mechanisms. Again, it is likely that sufficient lateral restraint is available at exterior boundaries through the action of compression rings [4]. This however is a matter of much greater importance than the restraint to thermal expansion as the survival of the floor system ultimately depends upon the reliability of the tensile membrane mechanism. This again is a key question for further investigation.

Another very important factor that has not been investigated here is the effect of the compartment geometry. This can have a large effect on the development of thermally induced forces and deflections in the heated structural members. The principle that allows one to make a quantitative assessment of the effect of compartment geometry, is **compatibility**. For instance for a rectangular fire compartment, the thermal expansion in the shorter direction will be smaller than the expansion the longer direction. This can lead to an increase in compression in the longer direction (because compatibility does not allow it to deflect as much as its thermal expansion demands). In the shorter the reverse happens, compatibility forces the deflections in this direction to be somewhat larger than thermal expansion would allow resulting in lower compressions or even tensile forces. This has been identified clearly in the modelling of the British Steel restrained beam test (3m$\times$8m) where the midspan ribs are in tension. This allows redistribution of the thermally induced forces.

10 Conclusions

The fundamental principles presented in this paper provide a means of estimating forces and displacements in real structures with appropriate idealisations. Such estimates can be of considerable use in assessing the results from more rigorous numerical analyses or they can be used in design calculations. Examples of such usage will be presented in a subsequent paper. There are however a considerable number of very important issues that remain to be investigated as mentioned in the previous section. Considerable effort is required to address these issues to satisfaction before a complete set of principles can be developed.

References

[1] J.M.Rotter, A.M.Sanad, A.S.Usmani, and M.Gillie. Structural performance of redundant structures under local fires. In *Interflam'99, 8th International Fire Science and Engineering Conference*, pages 1069–1080, Edinburgh, Scotland, 29 June - 1 July 1999.

[2] J.M.Rotter and A.S.Usmani. Fundamental principles of structural behaviour under thermal effects. In *Proceedings of the First International Workshop on Strutures in Fire*, Copenhagen, Denmark, June 2000.

[3] A.M.Sanad, J.M.Rotter, A.S.Usmani, and M.O'Connor. Composite beam in buildings under fire. 2000. Resubmitted after revision.

[4] Y.C. Wang. Tensile Membrane Action in Slabs and its Application to the Cardington Fire Tests. Technical report, Building Research Establishment, 1996. Paper presented to the second Cardington Conference 12-14 March 1996.